Epidermal growth factor receptor inhibition sensitizes renal cell carcinoma cells to the cytotoxic effects of bortezomib

Jiabin An[1] and Matthew B. Rettig[1,2]

[1]VA Greater Los Angeles Healthcare System-West Los Angeles and [2]David Geffen School of Medicine at University of California at Los Angeles, Los Angeles, California

Abstract

In renal cell carcinoma (RCC) models, maximal cytotoxicity of the proteasome inhibitor bortezomib is dependent on efficient blockade of constitutive nuclear factor κB (NF-κB) activity. Signaling through the epidermal growth factor receptor (EGFR) has been shown to result in NF-κB activation. Thus, we sought to investigate whether inhibition of the EGFR sensitizes RCC cells to the cytotoxic effects of bortezomib. We first established that constitutive NF-κB activity is dependent on signaling through the EGFR in RCC cells. Indeed, blockade of EGFR signaling with an EGFR tyrosine kinase inhibitor (TKI) resulted in inhibition of NF-κB activity. Using pharmacologic and genetic approaches, we also showed that EGFR-mediated NF-κB activation occurs through the phosphotidylinositol-3-OH kinase/AKT pathway. Combinations of the EGFR-TKI and bortezomib resulted in synergistic cytotoxic effects when RCC cells were pretreated with the EGFR-TKI, but an antagonistic interaction was observed with bortezomib pretreatment. Evaluation of the effects of drug sequencing on inhibition of NF-κB activity revealed that EGFR-TKI pretreatment markedly augmented the NF-κB inhibitory effect of bortezomib, whereas bortezomib preexposure resulted in suboptimal NF-κB blockade and thus provides a biochemical explanation for the drug interaction results. We conclude that the constitutive NF-κB activity observed in RCC cells is mediated, at least in part, through an EGFR/phosphotidylinositol-3-OH kinase/AKT signaling cascade. Pretreatment with an EGFR-TKI sensitizes to bortezomib-mediated cytotoxicity by inhibiting constitutive NF-κB activity. The combination of bortezomib and a currently approved EGFR inhibitor warrants clinical investigation. [Mol Cancer Ther 2007;6(1):61–9]

Introduction

An estimated 36,160 new cases of and 12,660 deaths from cancers of the kidney and renal pelvis are anticipated for the year 2005 (1). Metastatic renal cell carcinoma (RCC), which is present in ~30% of patients at the time of diagnosis and develops in one third of the remainder of patients who have clinically localized disease at presentation, is ultimately responsible for patient mortality (2). Although immunotherapies, including interleukin 2 and IFNα, have modest activity in RCC, the vast majority of patients are either primarily resistant to these treatments or relapse after an initial response (3–5). In fact, <5% of patients treated with high-dose interleukin 2 experience durable, complete remissions. In addition, immunotherapy is not typically offered to patients with non–clear cell histologies because of its lack of effect in this patient subpopulation (6). Moreover, metastatic RCC is quite resistant to chemotherapy, in large part due to high expression of the multidrug resistance gene (3–5). Accordingly, the median survival of metastatic RCC remains at only 8 months. Although two recently approved novel agents, sorafenib and sunitinib, have shown modest activity (7), novel and effective therapeutic agents are required to alter the natural history of metastatic RCC.

Bortezomib, a proteasome inhibitor that is approved for clinical use in cases of relapsed multiple myeloma, has been tested in two phase 2 clinical trials as a single agent in metastatic RCC. Although the combined objective response rate in these two trials was only ~10% (8, 9), we interpret these results to indicate that bortezomib has the potential to serve as an effective agent for metastatic RCC if the mechanism of bortezomib resistance can be identified. Modulation of resistance pathways could potentially result in significantly higher objective response rates.

It has been suggested that the transcription factor nuclear factor κB (NF-κB) represents a principal molecular target of bortezomib (10). NF-κB transcriptional activity inhibits apoptosis in most cell systems and drives proliferation, angiogenesis, and invasion and metastasis (5, 11–14). The activity of NF-κB is regulated by IκB, the NF-κB inhibitory protein that binds to and sequesters NF-κB family members in the cytoplasm. When the NF-κB pathway is activated, IκB is phosphorylated by IκB kinase, which phosphorylates IκB at serine residues 32 and 36 (11). Phosphorylated IκB is subjected to ubiquitination and proteasome-mediated degradation, which results in the translocation of NF-κB to the nucleus, where it functions as a transcription factor.

An increasing body of evidence has implicated a specific role for heightened NF-κB activation in the oncogenesis of many hematologic malignancies and solid tumors (15–17). The evidence for NF-κB activation in RCC is as follows. First, constitutive NF-κB activation has been observed in

many RCC cell lines (18, 19). Moreover, inhibition of NF-κB sensitizes RCC cells to tumor necrosis factor α (19), and tumor necrosis factor α–related apoptosis-inducing ligand (18). The *in vivo* evidence for the role of NF-κB in RCC is highlighted by a recent study demonstrating that heightened NF-κB activation is associated with development and progression of RCC in actual patients (20).

Recently, we showed that bortezomib induces apoptosis and inhibits constitutive NF-κB activity in RCC cell models (21). Moreover, by engineering RCC cells to maintain NF-κB activity in the face of bortezomib exposure, we formally established that inhibition of constitutive NF-κB is required for the maximal apoptotic effect of bortezomib (21), thereby confirming the relevance of NF-κB as a molecular target for bortezomib in RCC.

One of the genetic hallmarks of clear cell RCC, which comprise ∼85% of all RCC cases, is the mutation of the von Hippel-Lindau (*VHL*) tumor suppressor gene. Hereditary clear cell RCC cases that occur as a manifestation of the autosomal dominant von Hippel-Lindau syndrome are uniformly associated with germ line *VHL* gene mutations that affect one of the two *VHL* alleles. At the molecular level, VHL disease arises from somatic loss or inactivation of the remaining wild-type allele and thus conforms to the Knudson two-hit model. The importance of *VHL* mutations in the pathophysiology of clear cell RCC is underscored by the fact that up to 80% of sporadic cases manifest biallelic loss/inactivation at the *VHL* locus (*VHL*−/− tumors) as a consequence of gross genetic loss, nonsense and missense point mutations, and hypermethylation of the *VHL* promoter (22, 23).

We and others showed that *VHL* loss activates NF-κB (19, 24). In further studies, we have shown that *VHL* loss drives NF-κB activation by resulting in accumulation of hypoxia-inducible factor α (HIFα; ref. 25), a transcription factor that plays a central role in cellular responses to hypoxia (26). In turn, HIFα induces expression of transforming growth factor α, with consequent activation of an epidermal growth factor receptor (EGFR)/phosphotidylinositol-3-OH kinase (PI3K)/protein kinase B (AKT)/IκB-kinase α (IKKα)/NF-κB signaling cascade (25). Furthermore, RCC cells in which VHL protein expression has been restored are markedly more sensitive to the cytotoxic effects of bortezomib than their *VHL*−/− counterparts (27). Thus, given the importance of NF-κB as a molecular target of bortezomib, we sought to investigate whether EGFR inhibition would sensitize RCC cells to the cytotoxic effects of bortezomib.

Materials and Methods

Cell Lines and Reagents

The clear cell RCC cell lines, UOK121, 786-0, and UMRC6, were cultured in DMEM (Omega Scientific, Thousand Oaks, CA) plus 10% fetal bovine serum (Hyclone, Logan, UT) plus antibiotics (100 U/mL of penicillin and 100 μg/mL of streptomycin; Omega Scientific) in a humidified atmosphere containing 5% CO_2 in air.

Bortezomib was supplied by Millennium Pharmaceuticals, Incorporated (Cambridge, MA); the PI3K inhibitors (wortmannin and LY294002) were from Calbiochem; and the EGFR tyrosine kinase inhibitor (EGFR-TKI) PD153035 (28), was purchased from Calbiochem (La Jolla, CA). All reagents were dissolved in DMSO, the final concentration of which was maintained at 0.1% DMSO for all experiments.

Transient Transfections

Cells were plated at a density of 1×10^5 per well in a 24-well format and allowed to adhere overnight before transfection.

Inhibition of AKT. To inhibit AKT, we used a plasmid (pAKT-DN) with a kinase dead AKT transgene (AKT-DN; ref. 29). For transient transfections, the NF-κB− or CRE-driven reporter constructs (pκB-luc and pCRE-luc, BD Biosciences, Clontech, Mountain View, CA) along with the pAKT-DN plasmid were cotransfected with LipofectAMINE Plus (Invitrogen, Carlsbad, CA) according to the manufacturer's instructions. The pRL-SV40 plasmid was cotransfected to normalize for transfection efficiency. Protein was harvested 48 h posttransfection, and firefly and *Renilla* luciferase was measured with the Dual Luciferase Assay kit (Promega, Madison, WI). Transfections were done in triplicate. Total DNA was held constant with empty control vector in all transfection experiments. Normalized values are reported as the mean ± SD from triplicate transfections.

Experiments Involving Pharmacologic Inhibitors. Transient transfections of the pκB-luc plasmid were done as described in the preceding paragraph except that we normalized reporter gene expression to protein concentration as previously described (30). Three hours after transfection, fresh medium with or without inhibitor (i.e., PD153035, wortmannin, or LY2942002) was added.

Electrophoretic Mobility Shift Assay

Electrophoretic mobility shift assays (EMSA) were done as previously described (24). Briefly, cells were washed with cold PBS, and buffer A [10 mmol/L HEPES (pH 7.9), 1.5 mmol/L $MgCl_2$, 10 mmol/L KCl, 1 mmol/L DTT, 200 μmol/L phenylmethylsulfonyl fluoride, 1 μmol/L leupeptin, 1 μmol/L aprotinin, and 100 μmol/L EDTA] was then added before pulverization with a tissue grinder. Subsequently, nuclei were pelleted, lysed with buffer C [20 mmol/L HEPES (pH 7.9), 0.42 mol/L NaCl, 1.5 mmol/L $MgCl_2$, 0.2 mol/LEDTA, 25% glycerol, 1 mmol/L DTT, and 200 μmol/L phenylmethylsulfonyl fluoride], and then passed several times through a 25-gauge needle. Debris was removed by centrifugation.

Wild-type and mutant κB and Oct-1 oligonucleotide probes were purchased from Santa Cruz Biotechnology (Santa Cruz, CA). Fifteen micrograms of nuclear protein were combined with end-labeled, double-stranded oligonucleotide probe, 1 μg of poly(deoxyinosinic-deoxycytidylic acid) from Amersham Pharmacia Biotech (Piscataway, NJ), in a final reaction volume of 20 μL for 20 min at room temperature. The DNA-protein complex was run on a 4% nondenaturing polyacrylamide gel with 0.4× Tris-borate EDTA running buffer before subsequent autoradiography. Cold competition experiments were

UOK121　　　　　　　　　　**UMRC6**

PD153035 (μM)　　0　2　4　8　16　　　　0　2　4　8　16
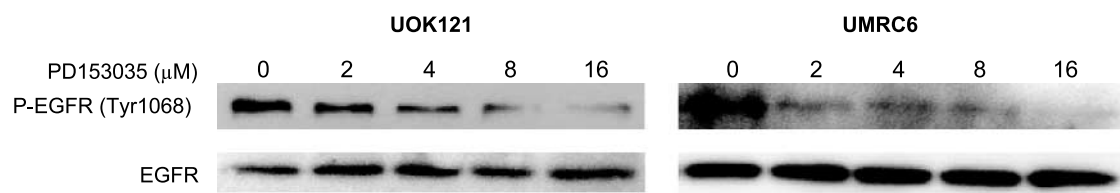
P-EGFR (Tyr1068)

EGFR

Figure 1. PD153035 inhibits EGFR activation. UOK121 and UMRC6 cells were exposed to PD153035 for 48 h. Whole-cell extracts were immunoprecipitated with an anti-EGFR antibody followed by immunoblotting with phosphospecific and total EGFR antibodies.

done with a 100-fold molar excess of double-stranded, cold wild-type or cold mutant κB oligonucleotide probes. As a control, EMSAs for Oct-1 were done in a similar manner.

Western Blots

Western blotting was done as previously described (21). Antibodies against phosphorylated AKT (pAKT; Thr[308]), pAKT (Ser[473]), total AKT, pEGFR (Tyr[1068]) and total EGFR were obtained from Cell Signaling Technology. The actin antibody was from Sigma (St. Louis, MO).

Cell Growth Assay

Cells were seeded in 96-well plates at 1.5×10^4 (UMRC6) and 1×10^4 (786-0 and UOK121) per well in 100 μL of culture medium. Cell viability was assessed by the 3,[4,5-dimethylthiazol-2-yl-]diphenyltatrazolium bromide (MTT) assay. Twenty-five microliters of MTT (5 mg/mL) were added to each well for 3 h at 37°C. Subsequently, 100 μL of 10% SDS/0.01 N HCl was added overnight at 37°C. Absorbance was measured at 570 nm on a microplate reader. All experiments were done in quadruplicate.

Median Effect/Combination Index Isobologram Method for Multiple Drug Effect Analysis

The effect of drug combinations on cytotoxicity was done by the median effect method using Calcusyn software, version 1.1.1 (Biosoft, Ferguson, MO; ref. 31). CI values were

calculated using the most conservative assumption of mutually nonexclusive drug interactions. CI values were calculated from median results of the MTT assays, which were done in quadruplicate. MTT values of vehicle-treated cells were normalized to 1. For the purpose of calculating CI values, the fraction affected (i.e., the fraction or proportion of cells that were inhibited by a given drug combination) was determined by the following calculation: fraction affected = 1 − MTT value. CI values significantly >1 indicate drug antagonism; CI values significantly <1 are indicative of synergy; and CI values not significantly different than 1 indicate an additive drug effect. Linear regression correlation coefficients of the median-effect plots were required to be >0.90 to show that the effects of the drugs follow the law of mass action, which is required for a median-effect analysis. For the purpose of CI calculations, the ratio of the molar concentrations of the two drugs (PD153035 and bortezomib) was held constant at 1:1.

Apoptosis and Cell Cycle Analyses. Apoptosis was measured by Annexin V-FITC staining (ApoAlert Annexin V-FITC Apoptosis kit, Clontech, Mountain View, CA) and flow cytometry. Cells were analyzed on a Becton Dickinson FACSCalibur flow cytometer with CellQuest software (BD Biosciences, San Diego, CA).

Cell cycle analysis was done by hypotonic propidium iodide staining. The propidium iodide staining buffer was
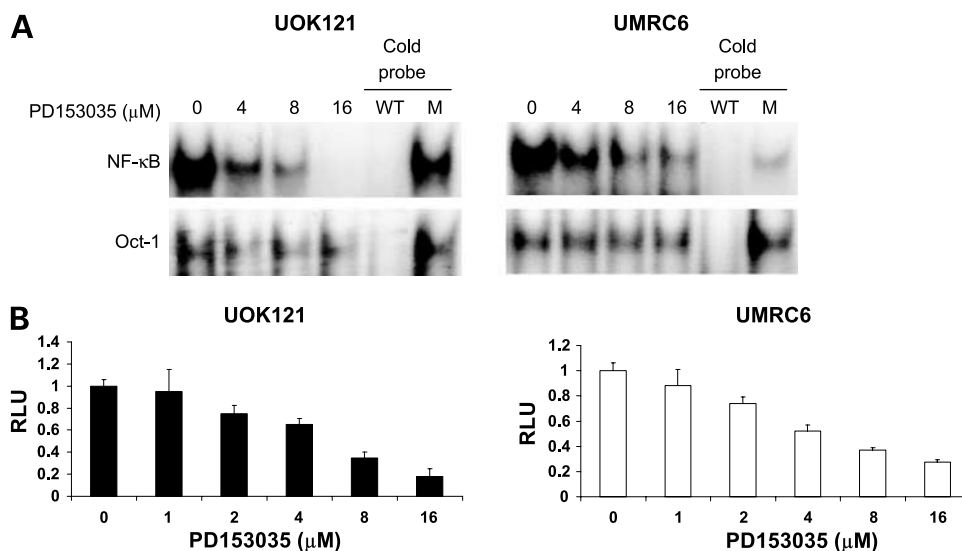
A　　　　　　　　**UOK121**　　　　　　　　　**UMRC6**

Figure 2. PD153035 inhibits constitutive NF-κB activity. UOK121 and UMRC6 cells were exposed to PD153035 for 48 h, and NF-κB activity was measured by EMSA-driven (**A**) and NF-κB–driven (**B**) reporter gene expression, reported as relative luminescence units (*RLU*), which were normalized to that of vehicle-treated cells. *Columns,* mean; *bars,* SD. **A,** cold competition experiments with cold wild-type (*WT*) or mutant (*M*) oligonucleotide probes.

freshly prepared in 250 mL of distilled water containing propidium iodide (0.025 g), sodium citrate (0.25 g), Triton X-100 (0.75 mL), and RNase A (5 mg). One milliliter of the propidium iodide staining buffer was added to 1×10^6 cells and placed on ice protected from light. Cells were analyzed on a Becton Dickinson FACSCalibur flow cytometer with CellQuest software.

Results

EGFR Inhibition Reduces Constitutive NF-κB Activity

Based on work by our group and others, it has been established that RCC tumor cells containing biallelic inactivating mutations of *VHL* (*VHL*−/−) manifest high constitutive NF-κB activity (19, 24). In addition, heightened NF-κB activation may occur through a pathway that requires EGFR activation (25). Thus, we first tested whether inhibition of constitutive EGFR activation results in down-regulation of NF-κB activity in *VHL*−/− clear cell RCC cell lines (UOK121 and UMRC6) that manifest constitutive HIF1α expression (32, 33). We exposed the HIF1α-expressing, *VHL*−/− clear cell RCC cell lines UOK121 and UMRC6 to increasing concentrations of PD153035, a selective EGFR-TKI (28). As shown in Fig. 1,

PD153035 inhibited EGFR activity in a dose-dependent manner as measured by Western blotting for phospho-EGFR. PD153035 did not affect the expression levels of total EGFR (Fig. 1, *bottom*).

Next, we showed that inhibition of the EGFR results in diminished NF-κB activity. Indeed, exposure to PD153035 led to a dose-dependent reduction in NF-κB activity as measured by EMSA and NF-κB–driven reporter gene expression (Fig. 2A and B, respectively). For the EMSAs, cold competition experiments confirmed the specificity of the shifted bands: Whereas excess cold wild-type NF-κB probe abrogated the shifted band, excess mutant probe did not affect band migration. PD153035 treatment had no effect on the results of an Oct-1 EMSA (Fig. 2A, *bottom*), thus confirming the specificity of the drug effect. As a negative control for the reporter assays, we found that PD153035 did not affect CRE-driven reporter gene expression (data not shown).

EGFR-Mediated NF-κB Activation Is Dependent on the PI3K/AKT Pathway

Because EGFR-mediated activation of NF-κB can occur through the PI3K/AKT pathway (25), we sought to confirm that EGFR and AKT activity were biochemically linked in HIF1α-expressing UOK121 and UMRC6 clear
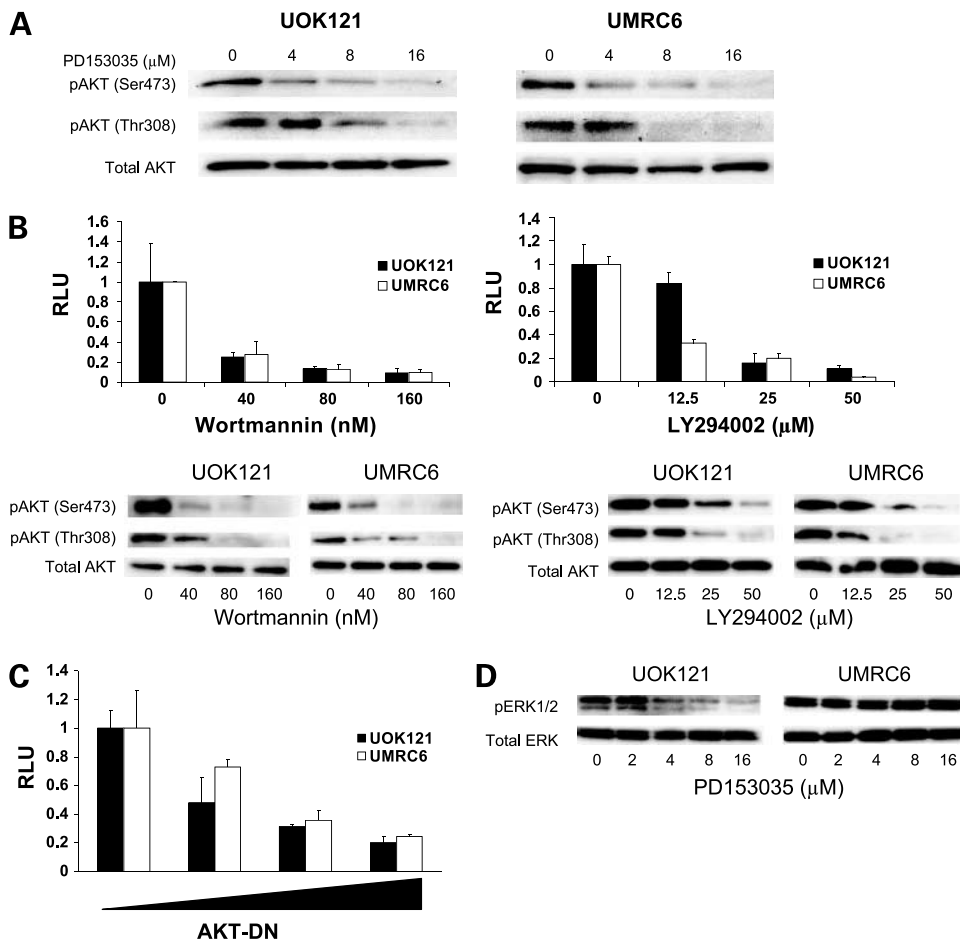

Figure 3. PD153035 inhibits NF-κB through the PI3K/AKT pathway. **A,** Western blot for phospho-AKT (Ser473 and Thr308) and total AKT. Whole-cell extracts were harvested after a 48-h exposure to PD153035 at the indicated concentrations. **B,** the PI3K inhibitors wortmannin and Ly294002 inhibit NF-κB–driven reporter gene expression. Inhibitors were added 3 h after transfection of the reporter, and protein was extracted after 48 h for reporter assays. *Bottom,* Western blots documenting inhibition of AKT phosphorylation by each PI3K inhibitor. **C,** inhibition of AKT with a kinase dead AKT-DN reduces NF-κB reporter activity. See Materials and Methods for details.
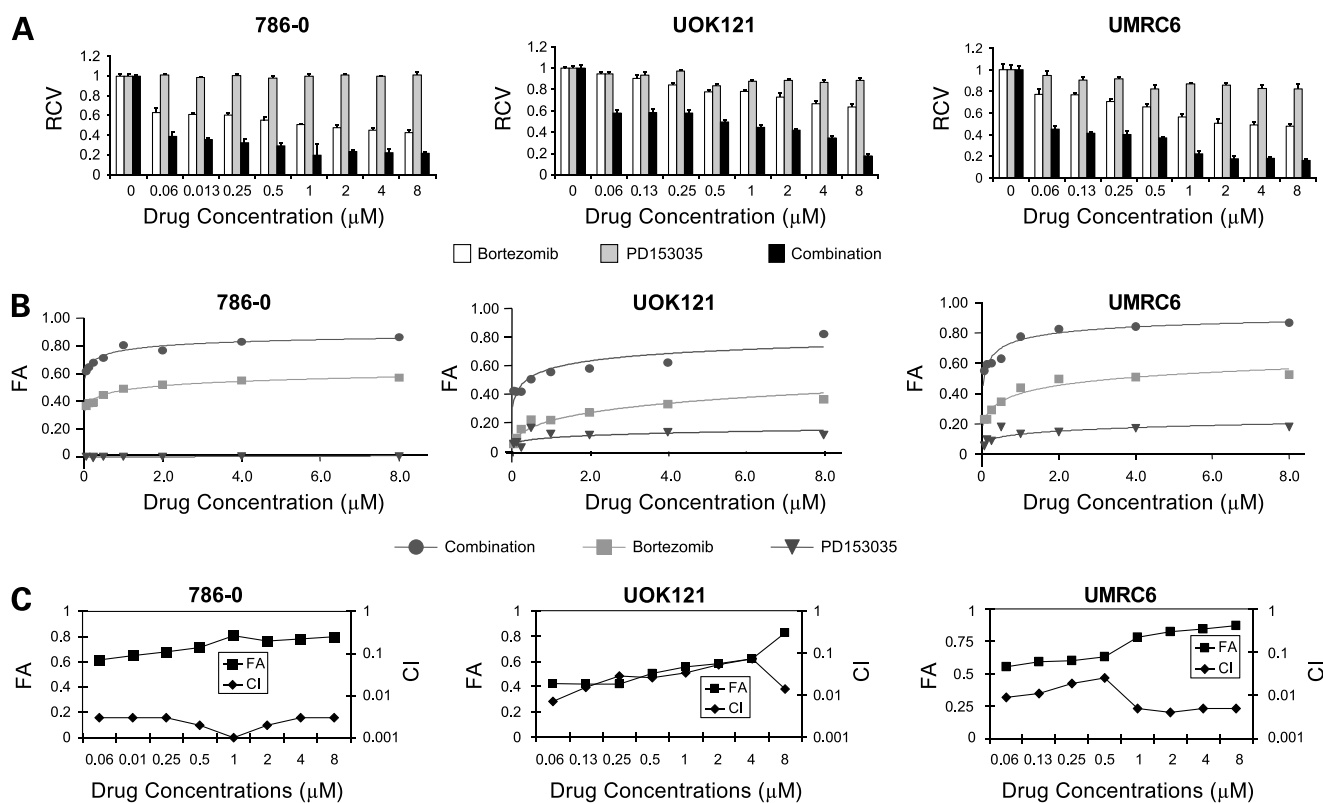
Figure 4. Growth-inhibitory effects of PD153035 and bortezomib alone or in combination. Cells were exposed to the indicated concentrations of PD153035 or bortezomib for 48 h before the MTT assay. **A,** relative cell viability (*RCV*) is reported such that vehicle-treated cells are assigned an RCV value of 1. *Columns,* RCV values; *bars,* SD. The same range of drug concentrations was used for both drugs. For drug combination experiments, cells were exposed to PD153035 for 2 h before the addition of bortezomib, and the ratio of the molar concentrations of the two drugs was held constant at 1:1. See Materials and Methods for details. **B,** graphical representation of data from **A.** *FA,* fraction affected (i.e., proportion of growth inhibition compared with vehicle-treated cells). **C,** CI analysis of MTT results presented in **A** and **B**. All CI values across the range of concentrations tested (0.0625 – 8 μmol/L) were statistically significantly less than 1 and therefore indicate synergistic drug interactions at these drug concentrations. See Materials and Methods for details.

cell RCC cells. When UOK121 and UMRC6 cells were exposed to increasing concentrations of PD153035, we observed a dose-dependent decrease in AKT activity as assayed by Western blotting with two different phospho-specific AKT antibodies (Fig. 3A). PD153035 had no effect on total AKT expression.

We next established that blockade of the PI3K/AKT pathway resulted in decreased NF-κB activity. Treatment of UOK121 and UMRC6 cells with the PI3K inhibitors wortmannin and LY204002 resulted in a dose-dependent inhibition of NF-κB–driven reporter gene expression (Fig. 3B). A kinase dead AKT dominant negative (AKT-DN) construct (29) likewise inhibited NF-κB–driven reporter gene expression in UOK121 and UMRC6 cells (Fig. 3C). As a control for the specificity of this effect, we showed that the AKT-DN construct had no effect on a CRE-driven reporter (not shown). Thus, EGFR-mediated NF-κB activation occurs in a PI3K/AKT–dependent manner in clear cell RCC cells that constitutively express HIF1α as a consequence of biallelic *VHL* loss.

Because the EGFR can signal through mitogen-activated protein kinase pathways, which may also activate NF-κB,

we explored the effects of EGFR blockade on the phosphorylation of extracellular signal-regulated kinase 1/2. Although PD153035 resulted in a dose-dependent inhibition of extracellular signal-regulated kinase 1/2 phosphorylation in UOK121 cells, EGFR inhibition did not affect the phosphorylation status of extracellular signal-regulated kinase 1/2 in UMRC6 cells (Fig. 3D). Consequently, inhibition of this mitogen-activated protein kinase pathway upon EGFR blockade is not a universal phenomenon in clear cell RCC cells; therefore, EGFR-induced activation of this mitogen-activated protein kinase cascade does not represent a common putative mechanism for

Table 1. Bortezomib IC_{50} values with and without PD153035 pretreatment

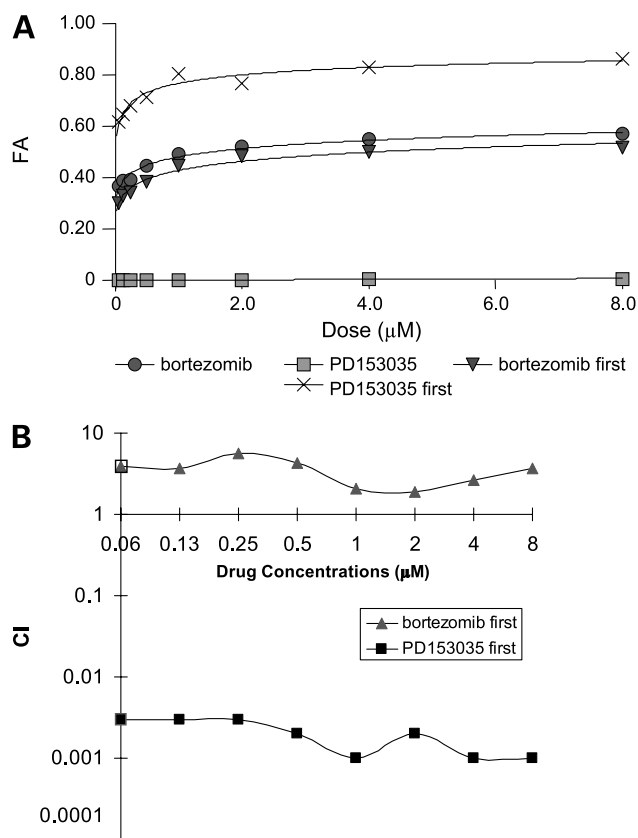|	Bortezomib (μmol/L)	PD153035 + bortezomib (nmol/L)
786-0	1.3	4.3
UOK121	3.5	55
UMRC6	18	3.8×10^2

Figure 5. Schedule-dependent effects on cell viability of the combination of PD153035 and bortezomib. 786-0 cells were exposed to PD153035 for 2 h before exposure to the combination of PD153035 and bortezomib for an additional 48 h (PD153035 first group) or the reverse (bortezomib first group) at the indicated concentrations. Cell proliferation and CI values were measured as in Fig. 4. **A,** graphical representation of data from drug interaction studies. **B,** graphical representation of CI values. Similar results were obtained for UOK121 and UMRC6 cells (not shown).

NF-κB activation. This finding is consistent with our previous report that activation of a Ras/Raf/extracellular signal-regulated kinase pathway did not affect NF-κB activity in *HIF2α*-expressing clear cell RCC cells (25).

Cytotoxic Effects of Bortezomib and PD153035 Alone and in Combination

Bortezomib as a single agent has activity against RCC cells *in vitro* (21, 24). Using the MTT assay to measure cellular growth of 786-0, UOK121, and UMRC6 cells, we confirmed this *in vitro* activity (Fig. 4). The concentrations of bortezomib required to inhibit the growth of these cell lines by 50% (IC_{50} values) were 1.3 μmol/L (786-0), 3.5 μmol/L (UOK121), and 18 μmol/L (UMRC6). Next, we examined the growth-inhibitory properties of PD153035 as a single agent. In all three clear cell RCC cell lines, PD153035 had little, if any, effect on overall growth, even up to a concentration of 8 μmol/L (Fig. 4).

In a previous report, we have shown that (*a*) bortezomib-induced cytotoxicity of RCC cell is NF-κB dependent (21) and (*b*) despite the ability of bortezomib to inhibit NF-κB

on its own, selective blockade of NF-κB sensitizes to bortezomib (24). This latter effect occurs because the NF-κB inhibitory effect of bortezomib is incomplete. Thus, we determined whether EGFR inhibition, by reducing basal levels of NF-κB activity, could sensitize RCC cells to the cytotoxic effects of bortezomib. When cells were pretreated with PD153035 for 2 h before adding bortezomib, we found that the cytotoxicity of bortezomib was markedly enhanced (Fig. 4A–B). To formally determine the nature of the drug interactions between PD153035 and bortezomib, we did combination index (CI) analysis, as previously described (31). For all three cell lines and across all concentrations tested (0.0625–8 μmol/L), there was a synergistic interaction between PD153035 and bortezomib as shown by CI values that were statistically significantly <1 (Fig. 4C). For example, pretreatment of 786-0 cells with the EGFR-TKI reduced the IC_{50} value of bortezomib from 1.4 μmol/L (bortezomib alone) to 4.3 nmol/L (combination of PD153035 and bortezomib; Table 1). Whereas the IC_{50} values for bortezomib alone were in the micromolar range, the IC_{50} values for the drug combination were in the nanomolar range/submicromolar range for all three clear cell RCC cell lines (Table 1).

Schedule Dependence of Effects of the Interaction between EGFR Inhibition and Bortezomib

We also tested whether the effects of the combination of PD153035 and bortezomib were affected by the timing of drug exposure. Synergy was not observed when cells were exposed to bortezomib before the EGFR-TKI; in fact, antagonism was observed (Fig. 5). Synergy was consistently observed as long as the EGFR-TKI exposure was either simultaneous or occurred first, and the duration of preexposure (2 h versus 24 h) did not influence the results (data not shown).

Because bortezomib is dependent on efficient blockade of NF-κB for its maximal cytotoxic effect (21, 24), we hypothesized that the antagonistic interaction observed when RCC cells were pretreated with bortezomib was related to incomplete NF-κB inhibition. Thus, we exposed RCC cells to the combination of PD153035 and bortezomib in different sequences. We found that pretreatment with PD153035 followed by bortezomib exposure markedly enhanced and virtually completely abolished NF-κB activity (Fig. 6A). This effect on NF-κB corresponded to the synergistic interaction observed when RCC cells were pretreated with PD153035 (Fig. 4). In contrast, pretreatment with bortezomib before PD153035 exposure resulted in significantly less NF-κB inhibition (Fig. 6A). Thus, the sequence of exposure to PD153035 and bortezomib clearly affects the overall level of NF-κB inhibition. The overall level of NF-κB blockade correlates with the degree of cytotoxicity induced by various sequences of exposure to the drug combination.

Because of our findings that NF-κB activation is AKT dependent in RCC cells (see above), we tested whether the sequencing of exposure to bortezomib and PD153035 also affected the degree to which these drugs inhibit AKT activation. Similar to the results for NF-κB blockade,

pretreatment of UOK121 cells with PD153035 before bortezomib exposure resulted in a more profound inhibition of phosphorylation of AKT than the effect of reversing the order of drug exposure or of either compound alone (Fig. 6B).

Given the known effects of NF-κB on genes that regulate survival and cell cycle progression, we investigated the effects of drug combinations on the induction of apoptosis and cell cycle profile. Similar to the MTT data (see Fig. 5), preexposure to PD153035 enhanced the proapoptotic effects of the drug combination (Fig. 7A, compare *panel 4* to other panels, especially *panel 5*). Cell cycle profile was analogously affected by drug sequencing. EGFR blockade before bortezomib treatment led to a profound arrest in G_2-M phase of the cell cycle (Fig. 7B, compare *panel 4* with *panel 5* and others).

Discussion

We have shown that EGFR blockade sensitizes clear cell RCC cells to the cytotoxic effects of the proteasome inhibitor bortezomib. In addition, constitutive NF-κB activity observed in HIF1α-expressing clear cell RCC cells is dependent on activation of the EGFR, which, in turn, signals through the PI3K/AKT pathway. These latter findings extend the results from our previous work that established the AKT dependence of EGFR-induced NF-κB activation in HIF2α-expressing clear cell RCC cells (25). The consistency in the AKT dependency of NF-κB activation between clear cell RCC cells that express HIF1α and HIF2α is critical because (*a*) RCC tumors may manifest expression of HIF1α and/or HIF2α (34) and (*b*) HIF1α and HIF2α induce different gene expression profiles that have the potential to differentially activate biochemical signaling pathways (35, 36).

Based on our prior work that established (*a*) the role of constitutive NF-κB activity in mediating bortezomib resistance in RCC cells (21) and (*b*) the dependence on

the EGFR signaling for basal NF-κB activity (25), we postulate that the principal mechanism whereby EGFR blockade results in heightened sensitivity to bortezomib is through inhibition of NF-κB activity. However, by blocking the proteasomal degradation of IκB, bortezomib by itself inhibits NF-κB activity (10, 37). Accordingly, one may ask why inhibition of NF-κB would enhance the cytotoxic effects of bortezomib. The answer lies in the fact that even at relatively high bortezomib concentrations, bortezomib-mediated NF-κB inhibition is incomplete in RCC cells (see Fig. 6; ref. 24). Moreover, we have shown that selective NF-κB blockade (i.e., by ectopic expression of an IκB ''super repressor'' or RNA interference of the NF-κB family member, p65) does in fact sensitize RCC cells to bortezomib (24). Thus, to achieve the maximum cytotoxic effect of bortezomib, we believe that NF-κB activity must be reduced below a critical threshold level, which typically cannot be accomplished in RCC cells through the NF-κB inhibitory effects of bortezomib alone.

The synergistic interaction between the EGFR-TKI, PD153035, and bortezomib is schedule dependent, such that the addition of the EGFR-TKI before bortezomib results in synergy, whereas reversing the order of drug exposure leads to drug antagonism. To account for this antagonism, we showed that preexposure to the EGFR-TKI results in virtually complete NF-κB blockade, whereas reversing the order of drug exposure leads to modest NF-κB inhibition. A similar dependence on drug sequencing was observed for AKT inhibition, a finding that is consistent with the AKT dependence of EGFR-induced NF-κB activation in clear cell RCC cells. We postulate that the diminished AKT and NF-κB inhibition observed when RCC cells were pretreated with bortezomib may result from decreased degradation of signaling proteins that function to converge on the EGFR/PI3K/AKT/NF-κB pathway, although direct evidence to support or refute this hypothesis warrants further investigation. Because the
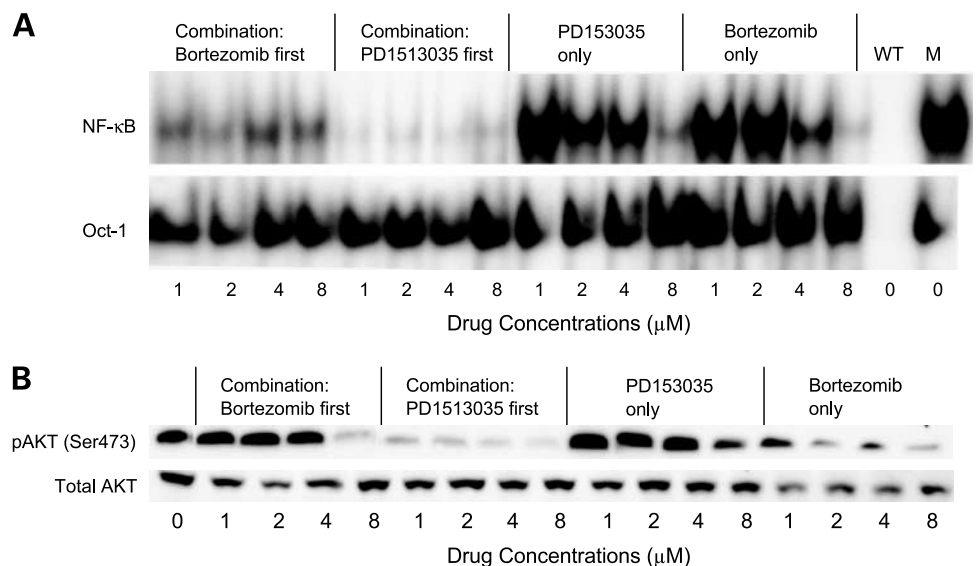

Figure 6. Schedule-dependent drug effects on NF-κB blockade and AKT activation. **A,** UOK121 cells were pretreated for 2 h with either PD153035 or bortezomib before exposure to the combination of the drugs for 24 h. Nuclear protein was harvested for EMSA analysis with NF-κB and Oct-1 probes. The Oct-1 EMSA represents a control to show specificity of the drug effects on NF-κB. At the far right of each EMSA are cold competition experiments with cold wild-type and mutant probes. **B,** UOK121 cells were treated as in **A.** Total cellular protein was extracted for Western blotting with the indicated antibodies.
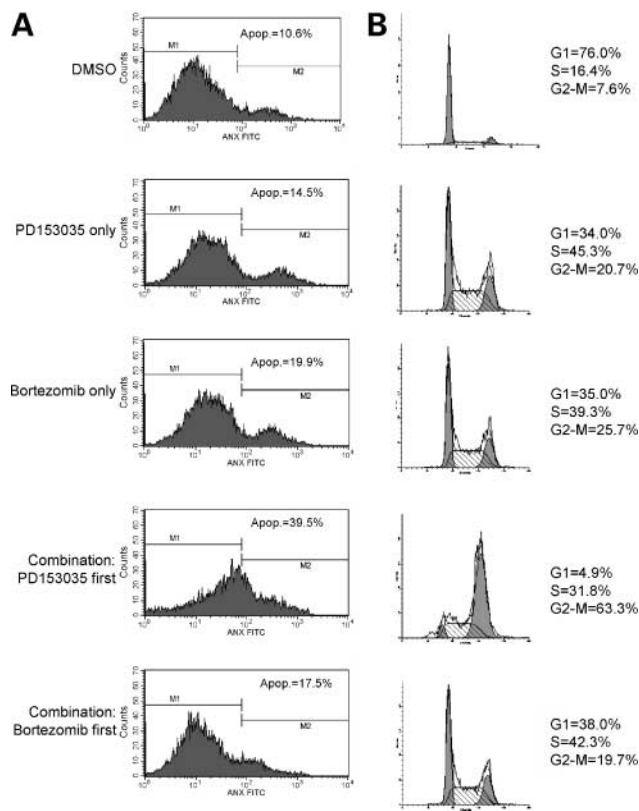
Figure 7. Schedule-dependent drug effects on apoptosis and cell cycle progression. UOK121 cells were treated as in Fig. 6 (except that drugs were used at a 4 μmol/L concentration only) and then analyzed for (**A**) apoptosis by Annexin V staining (percentage of apoptotic cells) or (**B**) cell cycle progression by hypotonic propidium iodide staining (percentage of cells in G_0-G_1, S, and G_2-M phases).

maximal cytotoxic effect of bortezomib is dependent on optimal NF-κB blockade (21, 24), it stands to reason that the differential effects of drug sequencing on NF-κB inhibition accounts for the synergistic versus antagonistic drug interactions that result depending on the timing of drug exposure.

Our findings of more profound induction of apoptosis and G_2-M arrest that was observed with EGFR blockade before bortezomib exposure is consistent with the role of NF-κB on driving the expression of genes that promote cell survival and cell cycle progression (11, 16, 38, 39). For example, NF-κB blockade has been previously shown to result in G_2-M arrest in cancer models other than RCC (40–42). Interestingly, selective inhibition of NF-κB typically does not result in apoptosis or reduced growth of solid tumor lines (43, 44), as we have previously shown to be the case for RCC (27). In contrast, selective inhibition of NF-κB activity does sensitize to apoptotic stimuli in numerous cell models (43, 44).

The absence of a significant *in vitro* effect of PD153035 is consistent with the lack of therapeutic activity of EGFR inhibitors as single agents in metastatic RCC patients (45–48). However, there may be clinical efficacy with a combination of EGFR blockade and bortezomib. For example, the IC_{50} values for bortezomib when cells were pretreated with PD153035 were in the nanomolar range (see Table 1), which is similar to the *in vitro* IC_{50} values for multiple myeloma and non–Hodgkin's lymphomas (IC_{50} values $\cong$1–50 nmol/L; refs. 49–51), diseases for which substantial clinical activity has been shown (52–54). A potential therapeutic trial of a drug combination of an EGFR-TKI and bortezomib is feasible. Based on our preclinical data, we propose that treatment of advanced RCC patients with an EGFR inhibitor would result in down-regulation of constitutive NF-κB activation that would sensitize to the cytotoxic effects of bortezomib.

Although this current study focused on targeting the EGFR as a means to reduce constitutive NF-κB activity for the purpose of enhancing the cytotoxicity of bortezomib, it is possible to choose alternative biochemical targets that drive NF-κB activation. These targets could be downstream of the EGFR, such as PI3K or AKT. With respect to the latter, drugs that inhibit a hyperactive AKT pathway could be successful in this regard and are currently in clinical development.

References

1. Jemal A, Murray T, Ward E, et al. Cancer statistics, 2005. CA Cancer J Clin 2005;55:10 – 30.

2. Waters WB, Richie JP. Aggressive surgical approach to renal cell carcinoma: review of 130 cases. J Urol 1979;122:306 – 9.

3. Glaspy JA. Therapeutic options in the management of renal cell carcinoma. Semin Oncol 2002;29:41 – 6.

4. Godley P, Kim SW. Renal cell carcinoma. Curr Opin Oncol 2002;14: 280 – 5.

5. Nathan PD, Eisen TG. The biological treatment of renal-cell carcinoma and melanoma. Lancet Oncol 2002;3:89 – 96.

6. Atkins MB, George D, Jonasch E. Medical management of renal cell carcinoma. In: UpToDate. Rose BD, editor. UpToDate. Wellesley, MA: 2006.

7. Patel PH, Chaganti RS, Motzer RJ. Targeted therapy for metastatic renal cell carcinoma. Br J Cancer 2006;94:614 – 9.

8. Davis NB, Taber DA, Ansari RH, et al. Phase II trial of PS-341 in patients with renal cell cancer: a University of Chicago phase II consortium study. J Clin Oncol 2004;22:115 – 9.

9. Kondagunta GV, Drucker B, Schwartz L, et al. Phase II trial of bortezomib for patients with advanced renal cell carcinoma. J Clin Oncol 2004;22:3720 – 5.

10. Mitchell BS. The proteasome—an emerging therapeutic target in cancer. N Engl J Med 2003;348:2597 – 8.

11. Baldwin AS, Jr. Series introduction: the transcription factor NF-κB and human disease. J Clin Invest 2001;107:3 – 6.

12. Guttridge DC, Albanese C, Reuther JY, Pestell RG, Baldwin AS, Jr. NF-κB controls cell growth and differentiation through transcriptional regulation of cyclin D1. Mol Cell Biol 1999;19:5785 – 99.

13. Yamamoto Y, Gaynor RB. Therapeutic potential of inhibition of the NF-κB pathway in the treatment of inflammation and cancer. J Clin Invest 2001;107:135 – 42.

14. Grumont RJ, Rourke IJ, Gerondakis S. Rel-dependent induction of A1 transcription is required to protect B cells from antigen receptor ligation-induced apoptosis. Genes Dev 1999;13:400 – 11.

15. Baldwin AS. Control of oncogenesis and cancer therapy resistance by the transcription factor NF-κB. J Clin Invest 2001;107:241 – 6.

16. Karin M, Cao Y, Greten FR, Li ZW. NF-κB in cancer: from innocent bystander to major culprit. Nat Rev Cancer 2002;2:301 – 10.

17. Rayet B, Gelinas C. Aberrant rel/NF-κB genes and activity in human cancer. Oncogene 1999;18:6938 – 47.

18. Oya M, Ohtsubo M, Takayanagi A, et al. Constitutive activation of nuclear factor-κB prevents TRAIL-induced apoptosis in renal cancer cells. Oncogene 2001;20:3888 – 96.

19. Qi H, Ohh M. The von Hippel-Lindau tumor suppressor protein sensitizes renal cell carcinoma cells to tumor necrosis factor-induced cytotoxicity by suppressing the nuclear factor-κB-dependent antiapoptotic pathway. Cancer Res 2003;63:7076 – 80.

20. Oya M, Takayanagi A, Horiguchi A, et al. Increased nuclear factor-κB activation is related to the tumor development of renal cell carcinoma. Carcinogenesis 2003;24:377 – 84.

21. An J, Sun Y, Fisher M, Rettig MB. Maximal apoptosis of renal cell carcinoma by the proteasome inhibitor bortezomib is nuclear factor-κB dependent. Mol Cancer Ther 2004;3:727 – 36.

22. Kondo K, Kaelin WG, Jr. The von Hippel-Lindau tumor suppressor gene. Exp Cell Res 2001;264:117 – 25.

23. Herman JG, Latif F, Weng Y, et al. Silencing of the VHL tumor-suppressor gene by DNA methylation in renal carcinoma. Proc Natl Acad Sci U S A 1994;91:9700 – 4.

24. An J, Fisher M, Rettig MB. VHL expression in renal cell carcinoma sensitizes to bortezomib (PS-341) through an NF-κB-dependent mechanism. Oncogene 2005;24:1563 – 70.

25. An J, Rettig MB. Mechanism of von Hippel-Lindau protein-mediated suppression of nuclear factor κB (NF-κB) activity. Mol Cell Biol 2005;25:7546 – 56.

26. Semenza GL. Targeting HIF-1 for cancer therapy. Nat Rev Cancer 2003;3:721 – 32.

27. An J, Fisher M, Rettig MB. VHL expression in renal cell carcinoma sensitizes to bortezomib (PS-341) through an NF-κB-dependent mechanism. Oncogene 2004;24:1563 – 70.

28. Fry DW, Kraker AJ, McMichael A, et al. A specific inhibitor of the epidermal growth factor receptor tyrosine kinase. Science 1994;265:1093 – 5.

29. Songyang Z, Baltimore D, Cantley LC, Kaplan DR, Franke TF. Interleukin 3-dependent survival by the Akt protein kinase. Proc Natl Acad Sci U S A 1997;94:11345 – 50.

30. Shen Y, Shenk T. Relief of p53-mediated transcriptional repression by the adenovirus E1B 19-kDa protein or the cellular Bcl-2 protein. Proc Natl Acad Sci U S A 1994;91:8940 – 4.

31. Chou TC, Talalay P. Quantitative analysis of dose-effect relationships: the combined effects of multiple drugs or enzyme inhibitors. Adv Enzyme Regul 1984;22:27 – 55.

32. Chen F, Kishida T, Duh FM, et al. Suppression of growth of renal carcinoma cells by the von Hippel-Lindau tumor suppressor gene. Cancer Res 1995;55:4804 – 7.

33. Gnarra JR, Zhou S, Merrill MJ, et al. Post-transcriptional regulation of vascular endothelial growth factor mRNA by the product of the VHL tumor suppressor gene. Proc Natl Acad Sci U S A 1996;93:10589 – 94.

34. Turner KJ, Moore JW, Jones A, et al. Expression of hypoxia-inducible factors in human renal cancer: relationship to angiogenesis and to the von Hippel-Lindau gene mutation. Cancer Res 2002;62:2957 – 61.

35. Sowter HM, Raval RR, Moore JW, Ratcliffe PJ, Harris AL. Predominant role of hypoxia-inducible transcription factor (Hif)-1α versus Hif-2α in regulation of the transcriptional response to hypoxia. Cancer Res 2003;63:6130 – 4.

36. Hu CJ, Wang LY, Chodosh LA, Keith B, Simon MC. Differential roles of hypoxia-inducible factor 1α (HIF-1α) and HIF-2α in hypoxic gene regulation. Mol Cell Biol 2003;23:9361 – 74.

37. Adams J. Potential for proteasome inhibition in the treatment of cancer. Drug Discov Today 2003;8:307 – 15.

38. Jin HS, Lee TH. Cell cycle-dependent expression of cIAP2 at G_2/M phase contributes to survival during mitotic cell cycle arrest. Biochem J 2006;399:335 – 42.

39. Deng L, Yang J, Zhao XR, et al. Cells in G_2/M phase increased in human nasopharyngeal carcinoma cell line by EBV-LMP1 through activation of NF-κB and AP-1. Cell Res 2003;13:187 – 94.

40. Raffoul JJ, Wang Y, Kucuk O, et al. Genistein inhibits radiation-induced activation of NF-κB in prostate cancer cells promoting apoptosis and G_2/M cell cycle arrest. BMC Cancer 2006;6:107.

41. Gatto S, Scappini B, Pham L, et al. The proteasome inhibitor PS-341 inhibits growth and induces apoptosis in Bcr/Abl-positive cell lines sensitive and resistant to imatinib mesylate. Haematologica 2003;88:853 – 63.

42. Pozarowski P, Halicka DH, Darzynkiewicz Z. Cell cycle effects and caspase-dependent and independent death of HL-60 and Jurkat cells treated with the inhibitor of NF-κB parthenolide. Cell Cycle 2003;2:377 – 83.

43. Kucharczak J, Simmons MJ, Fan Y, Gelinas C. To be, or not to be: NF-κB is the answer-role of Rel/NF-κB in the regulation of apoptosis. Oncogene 2003;22:8961 – 82.

44. Karin M, Yamamoto Y, Wang QM. The IKK NF-κB system: a treasure trove for drug development. Nat Rev Drug Discov 2004;3:17 – 26.

45. Dawson NA, Guo C, Zak R, et al. A phase II trial of gefitinib (Iressa, ZD1839) in stage IV and recurrent renal cell carcinoma. Clin Cancer Res 2004;10:7812 – 9.

46. Drucker B, Bacik J, Ginsberg M, et al. Phase II trial of ZD1839 (IRESSA) in patients with advanced renal cell carcinoma. Invest New Drugs 2003;21:341 – 5.

47. Motzer RJ, Amato R, Todd M, et al. Phase II trial of antiepidermal growth factor receptor antibody C225 in patients with advanced renal cell carcinoma. Invest New Drugs 2003;21:99 – 101.

48. Rowinsky EK, Schwartz GH, Gollob JA, et al. Safety, pharmacokinetics, and activity of ABX-EGF, a fully human anti-epidermal growth factor receptor monoclonal antibody in patients with metastatic renal cell cancer. J Clin Oncol 2004;22:3003 – 15.

49. Hideshima T, Richardson P, Chauhan D, et al. The proteasome inhibitor PS-341 inhibits growth, induces apoptosis, and overcomes drug resistance in human multiple myeloma cells. Cancer Res 2001;61:3071 – 6.

50. An J, Sun Y, Fisher M, Rettig MB. Antitumor effects of bortezomib (PS-341) on primary effusion lymphomas. Leukemia 2004;18:1699 – 704.

51. Pham LV, Tamayo AT, Yoshimura LC, Lo P, Ford RJ. Inhibition of constitutive NF-κB activation in mantle cell lymphoma B cells leads to induction of cell cycle arrest and apoptosis. J Immunol 2003;171:88 – 95.

52. Richardson PG, Barlogie B, Berenson J, et al. A phase 2 study of bortezomib in relapsed, refractory myeloma. N Engl J Med 2003;348:2609 – 17.

53. O'Connor OA. The emerging role of bortezomib in the treatment of indolent non-Hodgkin's and mantle cell lymphomas. Curr Treat Options Oncol 2004;5:269 – 81.

54. Orlowski RZ, Stinchcombe TE, Mitchell BS, et al. Phase I trial of the proteasome inhibitor PS-341 in patients with refractory hematologic malignancies. J Clin Oncol 2002;20:4420 – 7.

Epidermal growth factor receptor inhibition sensitizes renal cell carcinoma cells to the cytotoxic effects of bortezomib

Jiabin An and Matthew B. Rettig

Updated version	Access the most recent version of this article at: http://mct.aacrjournals.org/content/6/1/61

Cited articles	This article cites 52 articles, 23 of which you can access for free at: http://mct.aacrjournals.org/content/6/1/61.full#ref-list-1
Citing articles	This article has been cited by 8 HighWire-hosted articles. Access the articles at: http://mct.aacrjournals.org/content/6/1/61.full#related-urls

E-mail alerts	Sign up to receive free email-alerts related to this article or journal.
Reprints and Subscriptions	To order reprints of this article or to subscribe to the journal, contact the AACR Publications Department at pubs@aacr.org.
Permissions	To request permission to re-use all or part of this article, use this link http://mct.aacrjournals.org/content/6/1/61. Click on "Request Permissions" which will take you to the Copyright Clearance Center's (CCC) Rightslink site.